Enhanced Static Response of Sandwich Panels with Honeycomb Cores Through the Use of Stepped Facings

Cody H Nguyen, K Chandrahsekhara and Victor Birman

Journal of Sandwich Structures and Materials published online 24 June 2010
DOI: 10.1177/1099636210369615

Journal of Sandwich Structures and Materials OnlineFirst, published on June 24, 2010 as doi:10.1177/1099636210369615

JOURNAL OF SANDWICH STRUCTURES & MATERIALS

Original Article

Journal of Sandwich Structures and Materials
0(00) 1–24

DOI: 10.1177/1099636210369615
jsm.sagepub.com
SAGE

Enhanced Static Response of Sandwich Panels with Honeycomb Cores Through the Use of Stepped Facings

Cody H Nguyen[1], K Chandrashekhara[2] and Victor Birman[3]

Abstract

Sandwich panels have been developed to either produce lighter structures capable of carrying prescribed loads or to increase the load-carrying capacity subject to limitations on the weight. The major load-carrying elements of a sandwich structure are its facings, while the core primarily serves to resist transverse shear loads, enhance local strength and stability of the facings, and combine two facings into a single structural system. The facings being subject to in-plane tensile/compressive loads and to in-plane shear, their strength and stiffness are paramount to the sandwich structure. In this article we elucidate potential advantages of so-called 'stepped' facings with geometry modified to locally enhance the strength and stiffness at strategically important locations with a minimum effect on the weight. Numerous examples presented in the article validate our suggestion that a combination of a relatively simple manufacturing process and improved structural response of sandwich panels with stepped facings may present a designer with an attractive alternative to conventional sandwich structures.

Keywords

sandwich panel, strength, composite structures, variable stiffness

[1]Boeing, 163 J.S. McDonnell Blvd St. Louis, Missouri 63366, USA
[2]Department of Mechanical and Aerospace Engineering, Missouri University of Science and Technology (Formerly University of Missouri-Rolla), Rolla, Missouri 65409, USA
[3]Engineering Education Center, Missouri University of Science and Technology (Formerly University of Missouri-Rolla), One University Blvd., St. Louis, Missouri 63121, USA

Corresponding author:
Victor Birman, Engineering Education Center, Missouri University of Science and Technology (Formerly University of Missouri-Rolla), One University Blvd., St. Louis, Missouri 63121, USA
Email: vbirman@mst.edu

Introduction

Sandwich panels have to satisfy a number of requirements to their strength, stiffness, stability, and dynamic properties. These requirements can be met by enhancing the stiffness of the facings. This stiffness can be improved using one of the following methods:

1. Stiffer facing material with higher strength.
2. Functionally graded composite facings with variable in-plane or through the thickness properties (e.g., review by Birman and Byrd [1]).
3. Facings with a variable nonconventional geometry that could be called 'sculptured' facings.

Sculptured facings can be designed in a number of ways, but the goal is always to increase the stiffness, either locally at the location of highest bending stress couples or over the entire facing. Two possible designs are facings with a piece-wise thickness distribution shown in Figure 1 and ribbed facings with spaced stringers either embedded within the polymeric core or separating honeycomb sections placed in the space between the facings and the stringers [2]. In this article, we concentrate on the former design referred to as stepped facings. It should be noted that research on sandwich structures with a variable thickness has been conducted since the eighties [3–10]. However, these studies were concerned with tapered structures with a variable thickness of the core. Design considered here is concerned with the panel of a constant overall thickness that may be more feasible in numerous applications.

The panel with stepped facings shown in Figure 1 can easily be manufactured using honeycomb or polymeric core sections of various depths. In this article we concentrate on the 'global' response of the panel. The analysis of local stresses at the junction between sections of unequal face thickness that may affect local strength of the panel is outside the scope of the article. Note that these stresses may become essential in the case of polymeric cores, while the relevant effect for honeycomb core panels considered

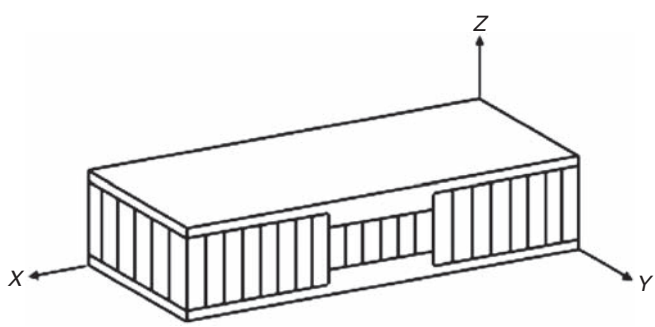

Figure 1. Honeycomb sandwich panel with stepped facings. The central section of the panel has thicker facings providing a higher local stiffness.

in the numerical analysis in this article should be less prominent. Accordingly, the present analysis and conclusions are relevant for honeycomb core panels, while their applicability to polymeric core structures requires additional analysis.

The purpose of this article is to estimate potential advantages of sandwich panels with stepped facings in static bending and stability problems. The approach to the solution includes the analytical part based on the first-order shear deformation theory and a numerical finite element solution utilizing 3D finite elements to model the core. The article elucidates improvements in strength and stiffness achieved using stepped facings, while monitoring an associated detrimental weight increase. This analysis results in conclusions on the desirability and feasibility of stepped facings. It is also shown that the first-order theory may be sufficiently accurate for the numerical analysis of sandwich panels with metallic honeycomb cores if they are not subject to local loads.

Analysis: Analytical formulation

The formulation of the problem for sandwich panels with piece-wise facings is based on the first-order shear deformation theory [11]. This is justified since aerospace panels presently considered for the application of stepped facings are relatively thin, so that the error produced by neglecting higher-order effects associated with warping of cross sections during deformation is negligible. The first-order theory was shown to yield accurate results for relatively slender sandwich panels if used with correct values of the shear correction coefficients [12]. It is usually accepted that the assumptions of the first-order shear deformation theory are sufficiently accurate for sandwich structures with a relatively stiff core [13].

It is emphasized that the first-order theory is definitely unacceptable for studies of problems involving local loads where 3D state of stress may be prevalent. For example, this theory would lead to serious mistakes if applied to the local stress analysis in the vicinity of bolts used to fasten the panel. In general, local stresses close to any discontinuity in the sandwich structure should be investigated by a higher-order theory or by a 3D theory of elasticity or plasticity (the latter theory may be needed if the facings are manufactured from ductile metal matrix composites or metals). The other situation where the first-order theory cannot be employed is found in sandwich structures with a 'soft' core. While a detailed discussion of the subject of sandwich structures with a soft core is outside the scope of this article, interested readers are referred to a number of recent references on the subject [13–15].

As follows from the previous paragraph, limitations superimposed on the use of the first-order theory are mostly irrelevant to problems considered in this article that are concerned with a 'global' response of sandwich panels. Moreover, panels considered in the present study have an aluminum honeycomb core that cannot be characterized as 'soft.' The validity of the theory will further be proven through a comparison of the results with those generated by FEA using 3D finite elements. In addition to the assumptions of the first-order theory, the problem considered here is geometrically linear. This simplification is justified since sandwich panels found

in typical applications fail at deflections that are smaller than the values necessitating the use of a geometrically nonlinear theory.

The solution of the static bending problem for a stepped panel simply supported along the straight edges $x = 0, a$, $y = 0, b$ and subjected to a lateral pressure $q(x, y)$ was obtained by the Rayleigh–Ritz method representing the potential energy as

$$\Pi = \frac{1}{2}\sum_{i,j}\int_{x_i}^{x_{i+1}}\int_{y_j}^{y_{j+1}}\int_{-h/2}^{h/2} u(x,y,z)\mathrm{d}z\mathrm{d}y\mathrm{d}x - \int_0^a\int_0^b q(x,y)w(x,y)\mathrm{d}y\mathrm{d}x \qquad (1)$$

where $u(x, y, z)$ is a strain energy density, w is a deflection of the panel, h is its thickness, and $x_i \le x \le x_{i+1}$, $y_j \le y \le y_{j+1}$ identify the section with a constant facing thickness. The overall thickness of the sandwich panel is constant, but the local thickness of the facings and the section of the core between these facings vary with in-plane coordinate as reflected in Figure 1. The sum in the first term in the right side of Equation (1) includes all sections of the panel. The integration in Equation (1) is conducted throughout the thickness accounting both for the contribution of the strain energy associated with in-plane stresses in the facings as well as for the transverse shear strain energy accumulated in the core.

The strain energy density of a material in the 3D state of stress in the Cartesian coordinate system is

$$u = \frac{1}{2}\left(\sigma_x\varepsilon_x + \sigma_y\varepsilon_y + \sigma_z\varepsilon_z + \tau_{xy}\gamma_{xy} + \tau_{xz}\gamma_{xz} + \tau_{yz}\gamma_{yz}\right), \qquad (2)$$

where σ_i and τ_{ij} denote axial and shear stresses, respectively, while ε_i and γ_{ij} are axial and shear strains. The simplifications introduced in the strain energy density of the facings and core modeled by the first-order shear deformation theory are illustrated in the subsequent analysis.

The stress-strain relationships for a generally orthotropic material relate the tensor of stresses to the tensor of strains [11]:

$$\begin{Bmatrix}\sigma_x\\ \sigma_y\\ \sigma_z\\ \tau_{yz}\\ \tau_{xz}\\ \tau_{xy}\end{Bmatrix} = \begin{bmatrix} C_{11} & C_{12} & C_{13} & 0 & 0 & C_{16}\\ C_{12} & C_{22} & C_{23} & 0 & 0 & C_{26}\\ C_{13} & C_{23} & C_{33} & 0 & 0 & C_{36}\\ 0 & 0 & 0 & C_{44} & C_{45} & 0\\ 0 & 0 & 0 & C_{45} & C_{55} & 0\\ C_{16} & C_{26} & C_{36} & 0 & 0 & C_{66}\end{bmatrix}\begin{Bmatrix}\varepsilon_x\\ \varepsilon_y\\ \varepsilon_z\\ \gamma_{yz}\\ \gamma_{xz}\\ \gamma_{xy}\end{Bmatrix}, \qquad (3)$$

where $[C]$ is a stiffness tensor.

According to the first-order theory approach to the analysis of sandwich structures [16], the facings are assumed in the state of plane stress, while the core is subject to transverse shear stresses. Furthermore, the thickness of the panel remains constant during deformation, that is, $\varepsilon_z = 0$. These simplifications yield stress-strain equations of the first-order theory for the facings and core, that is

$$\text{Facings:}\quad \begin{Bmatrix}\sigma_x\\ \sigma_y\\ \tau_{xy}\end{Bmatrix} = \begin{bmatrix}C_{11} & C_{12} & C_{16}\\ C_{12} & C_{22} & C_{26}\\ C_{16} & C_{26} & C_{66}\end{bmatrix}\begin{Bmatrix}\varepsilon_x\\ \varepsilon_y\\ \gamma_{xy}\end{Bmatrix}$$
$$\text{Core:}\quad \begin{Bmatrix}\tau_{yz}\\ \tau_{xz}\end{Bmatrix} = \begin{bmatrix}C_{44} & C_{45}\\ C_{45} & C_{55}\end{bmatrix}\begin{Bmatrix}\gamma_{yz}\\ \lambda_{xz}\end{Bmatrix} \tag{4}$$

Although Equation (4) are not new, they require a certain clarification when applied to honeycomb core panels. In such panels, the stress in the core should be determined using the stiffness terms evaluated accounting for the fact that honeycomb includes empty cells separated by thin material walls. Accordingly, the stiffness of the core is evaluated as an effective stiffness, rather than the actual stiffness of the material [17].

Following standard assumptions of the first-order shear deformation theory the strains are the following functions of displacements and rotations:

$$\begin{aligned}\varepsilon_x &= \frac{\partial u_0}{\partial x} + z\frac{\partial \psi_x}{\partial x}, \quad \varepsilon_y = \frac{\partial v_0}{\partial y} + z\frac{\partial \psi_y}{\partial y}, \quad \varepsilon_z = 0\\ \gamma_{xy} &= \frac{\partial u_0}{\partial y} + \frac{\partial v_0}{\partial x} + z\left(\frac{\partial \psi_x}{\partial y} + \frac{\partial \psi_y}{\partial x}\right)\\ \gamma_{xz} &= \frac{\partial w}{\partial x} + \psi_x, \quad \gamma_{yz} = \frac{\partial w}{\partial y} + \psi_y.\end{aligned} \tag{5}$$

In Equations (5), u_0, v_0 are middle plane displacements in the x- and y-directions, respectively, and ψ_x, ψ_y represent rotations of the cross section in the xz- and yz-planes, respectively.

Sandwich panels considered in this article have symmetric cross-ply or symmetric multi-layered angle-ply facings. The honeycomb core is modeled using its equivalent stiffness so that it behaves as a homogeneous orthotropic material. Furthermore, the facings being symmetric about the middle plane of the panel, in-plane displacements are uncoupled from deflections and rotations. Then integrating the strain energy density of the sandwich panel throughout the thickness of the facings and the core and using Equations (2), (3), and (5) we obtain

$$\begin{aligned}\Pi = \frac{1}{2}\sum_{i,j}\int_{x_i}^{x_{i+1}}\int_{y_j}^{y_{j+1}} &\left[\begin{aligned} &D_{11}^{(ij)}\left(\frac{\partial \psi_x}{\partial x}\right)^2 + 2D_{12}^{(ij)}\frac{\partial \psi_x}{\partial x}\frac{\partial \psi_y}{\partial y} + D_{22}^{(ij)}\left(\frac{\partial \psi_y}{\partial y}\right)^2\\ &+ D_{66}^{(ij)}\left(\frac{\partial \psi_x}{\partial y} + \frac{\partial \psi_y}{\partial x}\right)^2 + kA_{55}^{(ij)}\left(\frac{\partial w}{\partial x} + \psi_x\right)^2\\ &+ kA_{44}^{(ij)}\left(\frac{\partial w}{\partial y} + \psi_y\right)^2\end{aligned}\right]\mathrm{d}y\mathrm{d}x\\ &- \int_0^a\int_0^b qw\,\mathrm{d}y\mathrm{d}x,\end{aligned} \tag{6}$$

where A_{ii} and D_{ij} are extensional and bending stiffnesses, respectively, and k is a shear correction factor introduced to compensate for a difference between the actual (warped) shape of the corresponding cross section as a result of deformation and the first-order idealization assuming that the cross section remains plane.

The solution can be obtained representing deflections and rotations in double Fourier series that satisfy both kinematic and static boundary conditions, irrespectively of the variations in the thickness of the facings:

$$\begin{aligned} w &= \sum_m \sum_n W_{mn} \sin\frac{m\pi x}{a} \sin\frac{n\pi y}{b} \\ \psi_x &= \sum_m \sum_n F_{mn} \cos\frac{m\pi x}{a} \sin\frac{n\pi y}{b} \\ \psi_y &= \sum_m \sum_n P_{mn} \sin\frac{m\pi x}{a} \cos\frac{n\pi y}{b} \end{aligned} \tag{7}$$

Note that in the bending problem the fact that the stiffness of a sandwich panel with stepped facings varies over the surface, does not reduce the accuracy of the solution obtained using series (7) as long as they involve a sufficient number of terms. However, in the linear buckling problem, harmonics in (7) are decoupled and the solution may be inaccurate. This inaccuracy occurs because the mode shape of buckling of a conventional panel that may be accurately represented using one harmonics in (7) does not generally coincide with the mode shape of an otherwise identical panel with stepped facings. Accordingly, the analytical solution considered in the article is limited to bending problems.

The substitution of Equations (7) into (6) and integration yields

$$\begin{aligned} \Pi = \frac{1}{2} \sum_{i,j} \sum_{m,k,n,r} & \left[\begin{array}{l} \left(D_{11}^{(ij)} \frac{m\pi}{a}\frac{k\pi}{a} F_{mn}F_{kr} + 2D_{12}^{(ij)} \frac{m\pi}{a}\frac{r\pi}{b} F_{mn}P_{kr} + D_{22}^{(ij)} \frac{n\pi}{b}\frac{r\pi}{b} P_{mn}P_{kr} \right) A_{mnkr}^{(ij)} \\ + D_{66}^{(ij)} \left(\frac{n\pi}{b}\frac{r\pi}{b} F_{mn}F_{kr} + 2\frac{k\pi}{a}\frac{n\pi}{b} F_{mn}P_{kr} + \frac{m\pi}{a}\frac{k\pi}{a} P_{mn}P_{kr} \right) B_{mnkr}^{(ij)} \\ + kA_{55}^{(ij)} \left(\frac{m\pi}{a}\frac{k\pi}{a} W_{mn}W_{kr} + 2\frac{m\pi}{a} W_{mn}F_{kr} + F_{mn}F_{kr} \right) C_{mnkr}^{(ij)} \\ + kA_{44}^{(ij)} \left(\frac{n\pi}{b}\frac{r\pi}{b} W_{mn}W_{kr} + 2\frac{n\pi}{b} W_{mn}P_{kr} + P_{mn}P_{kr} \right) D_{mnkr}^{(ij)} \end{array} \right] \\ & - \sum_{m,n} W_{mn} \int_0^a \int_0^b q(x,y) \sin\frac{m\pi x}{a} \sin\frac{n\pi y}{b} \mathrm{d}y \mathrm{d}x, \end{aligned} \tag{8}$$

where

$$
\begin{aligned}
A_{mnkr}^{(ij)} &= \int_{x_i}^{x_{i+1}} \int_{y_j}^{y_{j+1}} \sin\frac{m\pi x}{a}\sin\frac{k\pi x}{a}\sin\frac{n\pi y}{b}\sin\frac{r\pi y}{b}\,\mathrm{d}y\mathrm{d}x \\
B_{mnkr}^{(ij)} &= \int_{x_i}^{x_{i+1}} \int_{y_j}^{y_{j+1}} \cos\frac{m\pi x}{a}\cos\frac{k\pi x}{a}\cos\frac{n\pi y}{b}\cos\frac{r\pi y}{b}\,\mathrm{d}y\mathrm{d}x \\
C_{mnkr}^{(ij)} &= \int_{x_i}^{x_{i+1}} \int_{y_j}^{y_{j+1}} \cos\frac{m\pi x}{a}\cos\frac{k\pi x}{a}\sin\frac{n\pi y}{b}\sin\frac{r\pi y}{b}\,\mathrm{d}y\mathrm{d}x \\
D_{mnkr}^{(ij)} &= \int_{x_i}^{x_{i+1}} \int_{y_j}^{y_{j+1}} \sin\frac{m\pi x}{a}\sin\frac{k\pi x}{a}\cos\frac{n\pi y}{b}\cos\frac{r\pi y}{b}\,\mathrm{d}y\mathrm{d}x.
\end{aligned}
\tag{9}
$$

The Rayleigh–Ritz procedure implies that $\frac{\partial \Pi}{\partial W_{mn}} = \frac{\partial \Pi}{\partial F_{mn}} = \frac{\partial \Pi}{\partial P_{mn}} = 0$ yielding the following system of algebraic equations for unknown amplitudes of harmonics in series (7):

$$
\begin{aligned}
&\sum_{i,j}\sum_{k,r}\left[kA_{55}^{(ij)}\left(\frac{m\pi}{a}\frac{k\pi}{a}W_{kr}+\frac{m\pi}{a}F_{kr}\right)C_{mnkr}^{(ij)}+kA_{44}^{(ij)}\left(\frac{n\pi}{b}\frac{r\pi}{b}W_{kr}+\frac{n\pi}{b}P_{kr}\right)D_{mnkr}^{(ij)}\right] \\
&-\int_0^a\int_0^b q(x,y)\sin\frac{m\pi x}{a}\sin\frac{n\pi y}{b}\,\mathrm{d}y\mathrm{d}x=0 \\
&\sum_{i,j}\sum_{k,r}\left[\begin{array}{l}\frac{m\pi}{a}\left(D_{11}^{(ij)}\frac{k\pi}{a}F_{kr}+D_{12}^{(ij)}\frac{r\pi}{b}P_{kr}\right)A_{mnkr}^{(ij)}+D_{66}^{(ij)}\frac{n\pi}{b}\left(\frac{r\pi}{b}F_{kr}+\frac{k\pi}{a}P_{kr}\right)B_{mnkr}^{(ij)} \\ +kA_{55}^{(ij)}\left(\frac{k\pi}{a}W_{kr}+F_{kr}\right)C_{mnkr}^{(ij)}\end{array}\right]=0 \\
&\sum_{i,j}\sum_{k,r}\left[\begin{array}{l}\frac{n\pi}{b}\left(D_{22}^{(ij)}\frac{r\pi}{b}P_{kr}+D_{12}^{(ij)}\frac{k\pi}{a}F_{kr}\right)A_{mnkr}^{(ij)}+D_{66}^{(ij)}\frac{m\pi}{a}\left(\frac{k\pi}{a}P_{kr}+\frac{r\pi}{b}F_{kr}\right)B_{mnkr}^{(ij)} \\ +kA_{44}^{(ij)}\left(\frac{r\pi}{b}W_{kr}+P_{kr}\right)D_{mnkr}^{(ij)}\end{array}\right]=0.
\end{aligned}
\tag{10}
$$

Upon solution of the system of Equations (10), the strains throughout the panel can be determined from Equations (5) and the stresses from Equations (4). If the maximum deflection of the panel exceeds its half-thickness, geometrically nonlinear terms should be included into formulation (in such case, the analysis should be conducted numerically). In the presence of local loads, such as pressure concentrated over a small area of the loaded facing, the present solution may provide global deformations and stresses. However, if the local load is large it is advisable to consider local deformations of the loaded facing and the sections of the core and the opposite facing in the loaded region. Besides, local geometrically nonlinear effects may result in an interaction between global and local deformations and stresses. Accordingly, such problems are better analyzed by numerical methods accounting for 3D and nonlinear effects.

The solution shown above is concerned with static pressure. In the case of eigenvalue problems, that is, buckling or free vibration, the approach is similar, but it is

necessary to account for the contribution of relevant energy terms. As indicated above, the accuracy of the linear analysis that limits the mode shape of buckling or vibration to one harmonics in series (7) may be insufficient. However, it is possible to obtain an accurate solution for forced response of the panel subject to dynamic pressure $q(x, y, t)$ where t is time. In this case, the amplitudes of harmonics in series (7) depend on time, and the kinetic energy should be added to the right side of (6):

$$K = \frac{1}{2}\sum_{i,j}\int_{x_i}^{x_{i+1}}\int_{y_j}^{y_{j+1}}\left[m\left(\frac{\partial w}{\partial t}\right)^2 + I\left(\left(\frac{\partial \psi_x}{\partial t}\right)^2 + \left(\frac{\partial \psi_y}{\partial t}\right)^2\right)\right]\mathrm{d}y\mathrm{d}x, \tag{11}$$

where

$$m = \int_z \rho(x, y, z)\mathrm{d}z \quad I = \int_z \rho(x, y, z)z^2\mathrm{d}z. \tag{12}$$

The Rayleigh–Ritz method applied to such problem of forced vibrations results in a system of ordinary differential equations with respect to the amplitudes of harmonics in Equation (7) that can be solved analytically or numerically dependent on the load–time relationship.

Analysis: Finite element model and numerical results

The model of the panel was developed using Nastran-2005. The facings were modeled by 2D shell elements, while the core consisted of 3D solid elements. The material of the cross-ply symmetric facings was laminated carbon/epoxy (T300/5208). The aluminum (AL-5056) honeycomb core was hexagonal with the foil thickness equal to 0.001 inch. The equivalent moduli of elasticity of the hexagonal core in the L and W directions were equal to 70.0 and 28.0 ksi, respectively, while the modulus in the direction perpendicular to the plane of the panel was 185 ksi (http://www.hexcel.com/Products/Core%2BMaterials/) Note that hereafter, the longer dimension of the panel is along the x-axis and the shorter edges are oriented along the y-axis.

First, the analytical solution for various conventional panel geometries (facings of constant thickness) was compared to the FEA result to verify the accuracy of the model. The chosen values of the shear correction factor employed in this analysis was 5/6 and 1.0 (the former value is typical in the first-order theory, while the latter value was recommended for sandwich structures in [18]). The difference between the results generated using these values of the shear correction factor was negligible. The size of panels considered in this comparison is listed in Table 1. The width-to-thickness ratio equal to 20 was maintained in all cases. The facings were symmetric and cross-ply laminated $[0^\circ/90^\circ/0^\circ/90^\circ]_s$. The thickness of each layer in the facings of panels considered in this study was equal to 0.127 mm (0.005″).

Table 1. Maximum deflections in conventional panels with the width-to-thickness ratio equal to 20 by the analytical first-order theory solution and 3D FEA.

Panel No.	Length in the *x*-direction, *a* (in.)	Length in the *y*-direction, *b* (in.)	Thickness, *h* (in.)	Depth of honeycomb core (in.)	Max deflection by first order theory (in.)	Max deflection by 3D FEA (in.)
1	20	10	0.50	0.42	0.176	0.169
2	24	12	0.60	0.52	0.232	0.224
3	28	14	0.70	0.62	0.296	0.287
4	32	16	0.80	0.72	0.368	0.358
5	36	18	0.90	0.82	0.447	0.436
6	40	20	1.00	0.92	0.535	0.522

Table 2. Maximum stresses in the layers of the compressed facing of a conventional panel (10″ long, 5″ wide and 1″ deep) by the analytical first-order theory solution and 3D FEA.

Layer (from surface to the core)	Orientation of layer (deg.)	Analytical σ_x, (ksi)	FEA σ_x, (ksi)	Difference between analytical and FEA deflections (%)	Analytical σ_y, (ksi)	FEA σ_y, (ksi)	Difference between analytical and FEA deflections (%)
8	0	38.989	38.572	1.07	3.644	3.673	0.80
7	90	2.866	2.935	2.41	51.137	52.533	2.73
6	0	38.208	37.588	1.62	3.294	3.394	3.04
5	90	2.807	2.809	0.07	47.452	47.842	0.82
4	90	2.779	2.746	1.19	44.555	45.497	2.11
3	0	37.039	36.112	2.50	3.041	2.975	2.17
2	90	2.720	2.260	3.68	43.627	40.806	6.47
1	0	36.259	35.128	3.12	2.977	2.696	9.44

Note: The sign minus indicating compression is omitted. Layer 8 is on the outer surface of the panel, while layer 1 is adjacent to the core.

The panels were loaded by a uniform pressure of 50 psi. The fact that numerical and analytical solutions were in close agreement, even for the width-to-thickness ratio of 20, can be attributed to the honeycomb core being relatively 'stiff.' Furthermore, the stresses in the compressed facing of an eight-layer facing panel that is 254 mm (10″) long, 127 mm (5″) wide, and 25.4 mm (1″) thick and subject to a uniform pressure of 350 psi were calculated by the first-order theory and compared with the 3D finite element solution (Table 2). As follows from this table, the error associated

with the first-order theory increases in the layers that are close to the core. However, even at the width-to-thickness ratio equal to 5, this error remains relatively small. Thus, the analytical solution (for metallic honeycomb core panels with the width-to-thickness ratio equal to or exceeding 20) probably does not have to rely on theories accounting for a 'soft' core, with the exception of the case of high local loads.

The following results were generated using FEA for simply supported panels that were 254 mm (10″) long, 127 mm (5″) wide, and 25.4 mm (1″) thick. Each facing of a 'conventional' panel referred to below included eight cross-ply layers. The facings of three-stepped panels included the central 12-layer $7.5'' \times 2.3''$ section, adjacent eight-layer section with the outer dimensions $8.5'' \times 3.5''$, and the outer six-layer section (Figure 2). The weight of the stepped panel was only 5.7% larger than that of the conventional counterpart. The bending load applied to the panel in the examples, except for the buckling analysis discussed below, was represented by a uniform static pressure equal to 2.413 MPa (350 psi).

The shapes of the conventional and stepped panels undergoing a uniform static pressure are shown in Figure 3. The contours of bent panels are depicted in Figures 4 and 5. As follows from these figures, the mode shapes of panels subject to static pressure are little affected by the stepped facing design.

The distribution of strains throughout the thickness of the panel with stepped facings is shown in Figure 6. In this and following figures and tables the strains and stresses are shown at the center of the panel where they are maximum, unless indicated otherwise. As follows from this figure, the axial strains in the x-direction

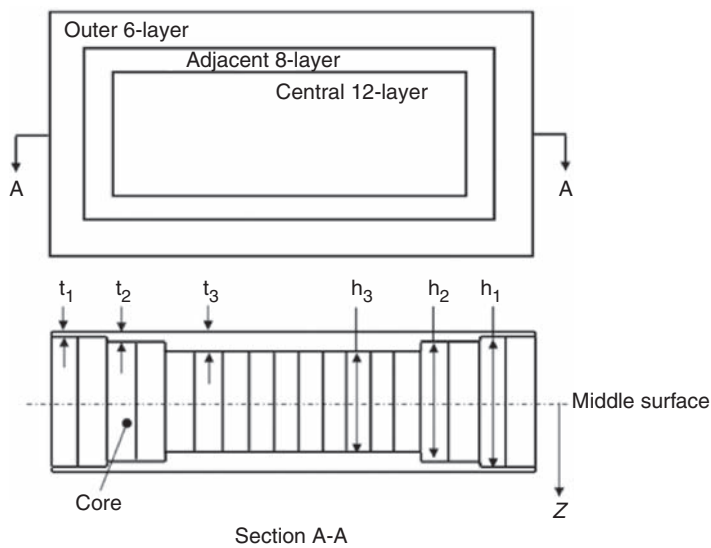

Figure 2. Schematic illustration of a sandwich panel with three-stepped facings.

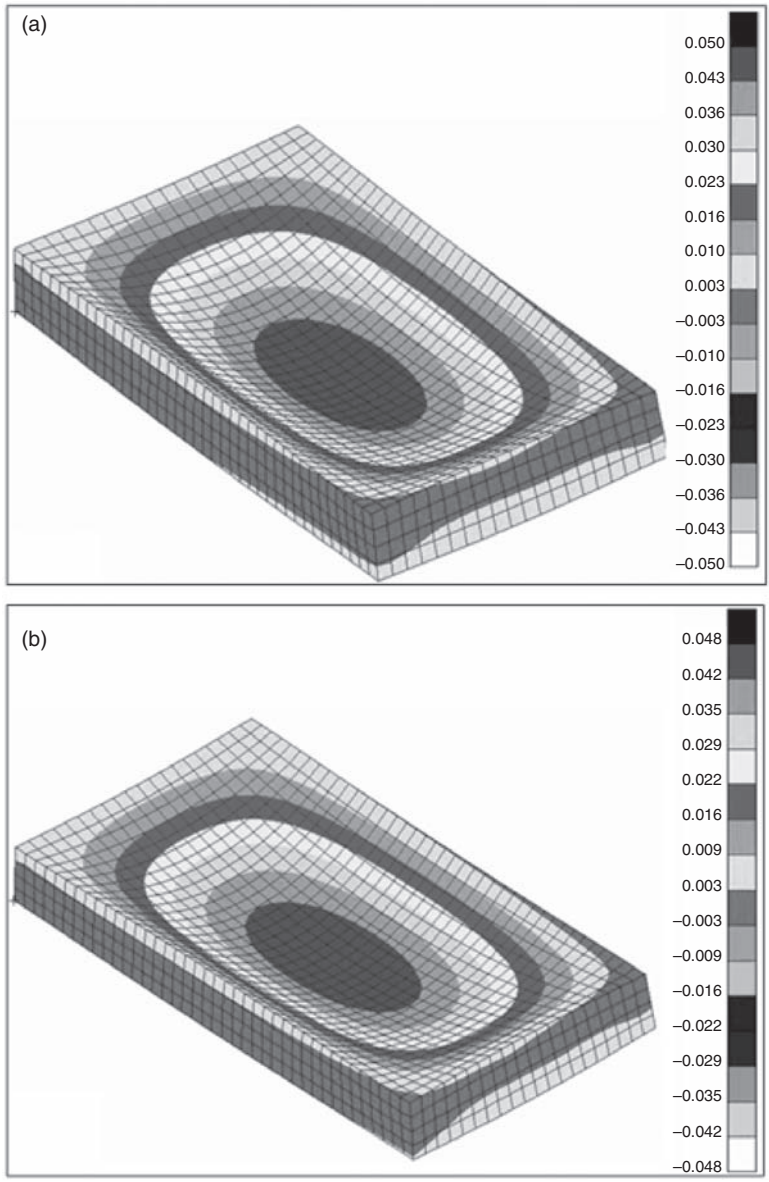

Figure 3. Shape of conventional (a) and stepped (b) panels undergoing bending due to a uniform pressure.

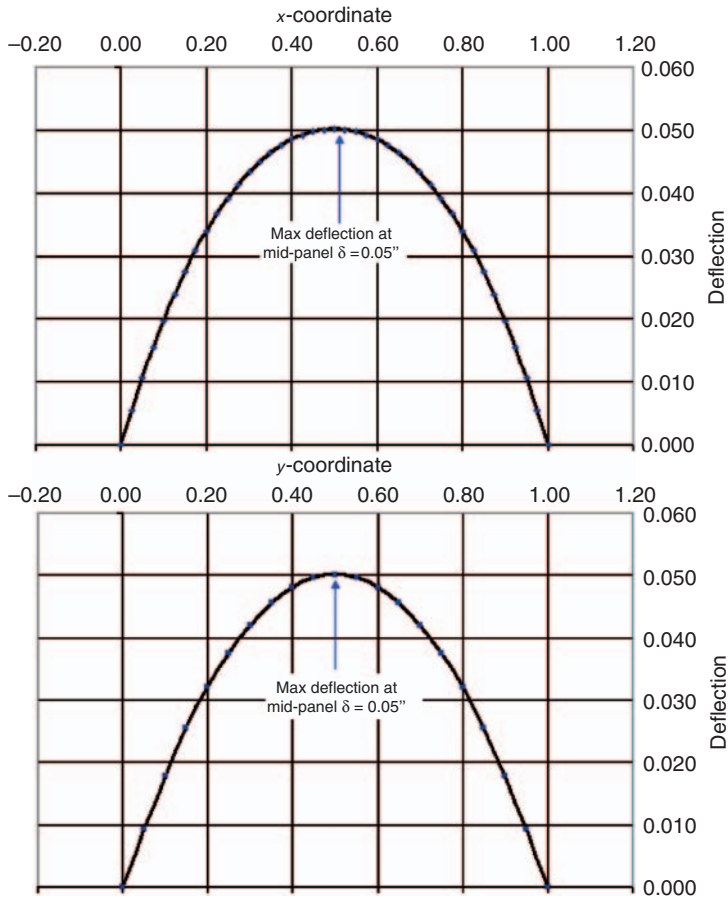

Figure 4. Mode shape of deflections of the conventional panel subject to a uniform pressure (the horizontal axes show nondimensional x- and y-coordinates normalized with respect to the corresponding dimension).

(ε_x) are nearly linearly distributed throughout the thickness. However, their counterparts in the y-direction (ε_y) deviate from the linear distribution, reflecting a small width-to-thickness ratio equal to 5. Evidently, the panels with such width-to-thickness ratio should be investigated using a higher-order theory or numerical FEA 3D models. It is interesting to note that while the strain in the y-direction is a nonlinear function of the thickness coordinate, a popular third-order theory would probably be insufficient to accurately represent its through-the-thickness distribution.

The effect of the stepped facing design on the strains and stresses in the panel compared to those in the conventional counterpart is depicted in Figures 7 and 8. As shown in Figure 7, the axial strains in the facings in both x- and y-directions are significantly reduced using stepped facings. Axial stresses in the facings are also

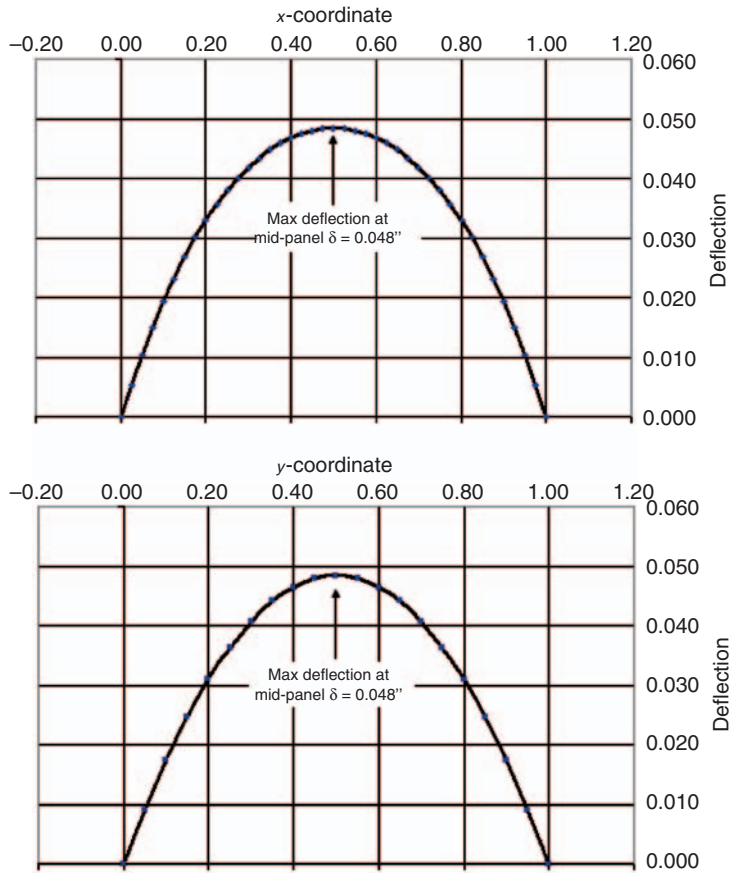

Figure 5. Mode shape of deflections of the stepped panel subject to a uniform pressure (the horizontal axes show nondimensional x- and y-coordinates normalized with respect to the corresponding dimension).

noticeably reduced by redistributing the material as follows from Figure 8. Note that while the strains are continuous functions of the thickness coordinate, the stresses in the facings change abruptly from layer to layer (this is evident in Figure 8). This reflects a much higher stiffness of layers of cross-ply facings in the fiber direction as compared to the stiffness of the same layers in the direction perpendicular to the fibers. The effect of stepped facing design on transverse shear stresses in the core is not shown since these stresses remained relatively small in all examples and they did not represent the mode of failure.

The comparison between the compressive stresses and strains at the center of the conventional (eight-layer facings) and stepped panels is also shown in Tables 3 and 4. This comparison is limited to the top facing that experiences compression as a result of bending. Note that while the tensile strains in the opposite facings have the

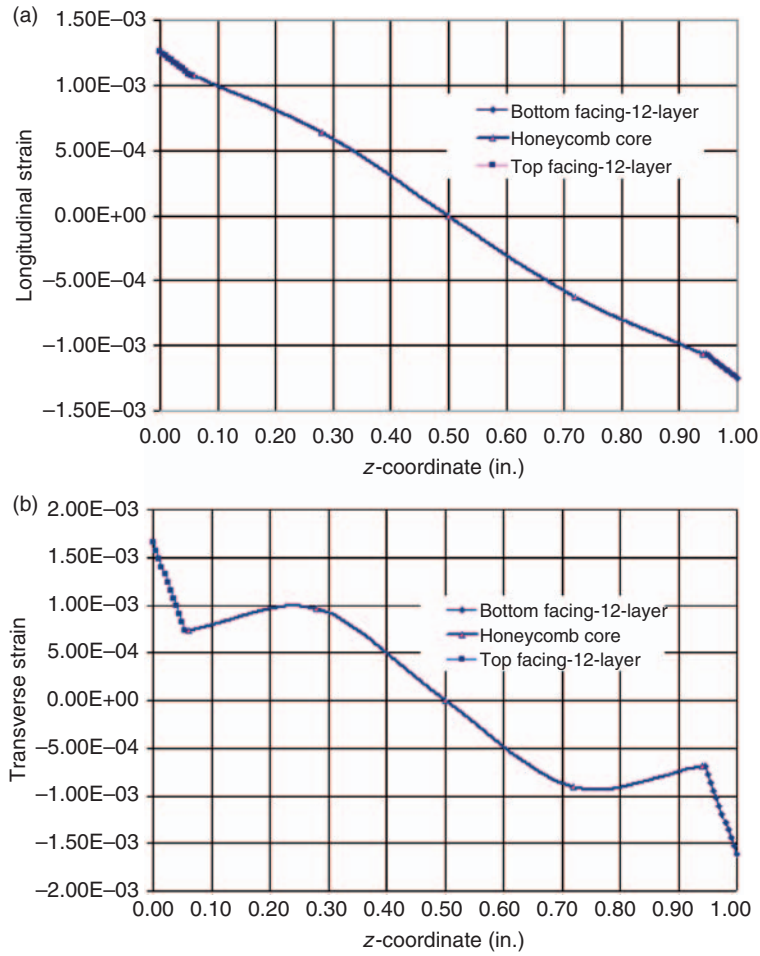

Figure 6. Distribution of axial strains throughout the thickness of stepped panels obtained by FEA: (a) strains in the x-direction, (b) strains in the y-direction.

same absolute value as those in the corresponding layers in the top facing, the stresses in the facings differ, reflecting a difference in the tensile and compressive moduli of the facing material. As follows from Figure 7 and 8 and from Table 3 and 4, a reduction in maximum stresses in the 0°-layers oriented in the x-direction reaches 12.9% in the fiber direction and 20.2% in the direction perpendicular to the fibers. For 90°-layers oriented in the y-direction the corresponding improvements in the maximum stress are 22.3% and 15.5%, respectively. The axial strains in the x-direction are also reduced by almost 13%. These improvements achieved at the cost of a small weight increase (5.7%) indicate that the use of stepped facings may be an attractive option in designs where the strength of the panel is the dominant factor.

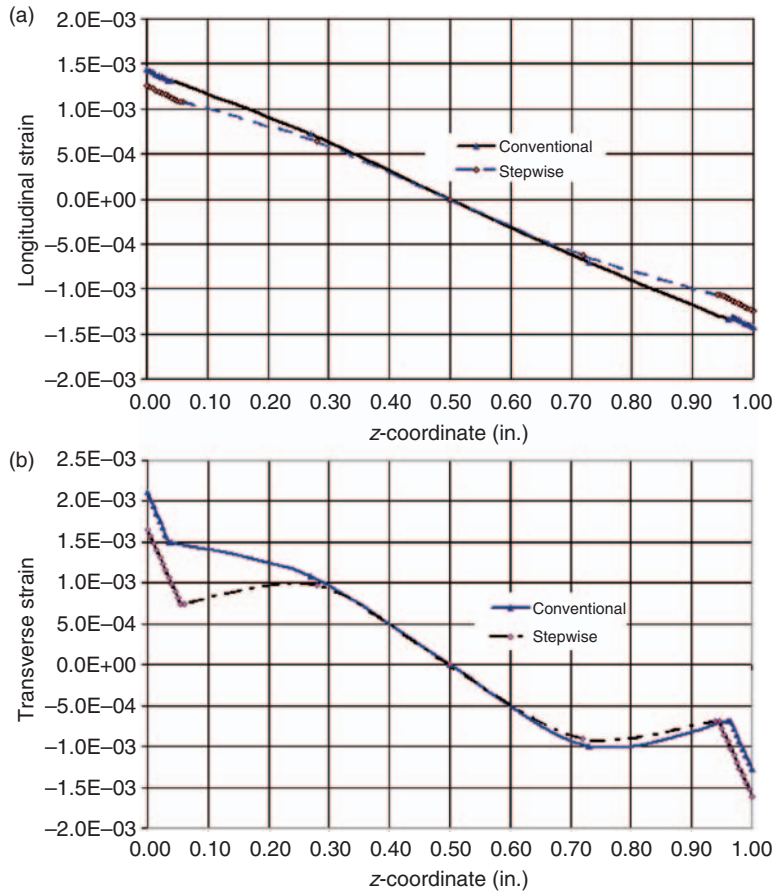

Figure 7. Distribution of axial strains throughout the thickness of conventional & stepped panels obtained by FEA: (a) strains in the x-direction, (b) strains in the y-direction.

Buckling resistance of sandwich panels can also be improved by the stepped facing design. This was demonstrated analyzing the panel subject to a uniform compression along the x-axis. The same stepped design as that described above resulted in an increase of the buckling load by 11.7% (from 3690 lbs to 4120 lbs). Note that the shape of the buckled panel was dominated by the first mode shape of deformation, i.e. one half-wave of deformation in both x- and y-directions. This mode shape was not noticeably different from the mode shape of buckling of the otherwise identical conventional panel.

A further insight into potential advantages of stepped facings is illustrated on the example of the panel with three-stepped facings (Figure 2) that was even more efficient than the previously considered panel. The overall dimensions of the sandwich panel and the materials of the facings and the honeycomb core were identical to those considered in the previous examples. The outer region of the panel

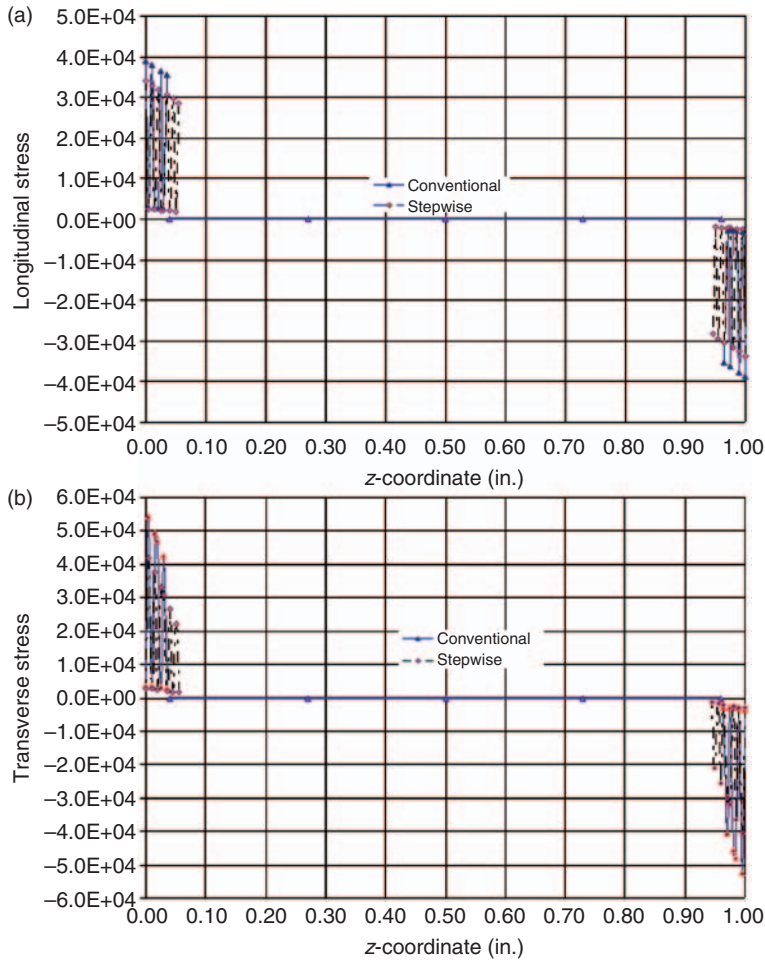

Figure 8. Distribution of axial stresses throughout the thickness of conventional & stepped panels obtained by FEA. (a) stresses in the x-direction, (b) stresses in the y-direction.

(see the region with thickness t_{f1} in Figure 2) was constructed of the facings with five cross-ply layers [0°/90°/0°/90°/0°]. The facings of the adjacent region (thickness t_{f2}) included seven layers, that is, [0°/90°/0°/90°/0°/90°/0°]. The facings in the thickest central region (thickness t_{f3}) consisted of 11 layers: [0°/90°/0°/90°/0°/90°0°/90°/0°/90°/0°]. The size of the central thicker facing region was $8.0'' \times 3.5''$, while the outer dimensions of the region with 7-layer facings were equal to $9.0'' \times 4.0''$. The weight of this stepped panel was only 3.1% more than that of the conventional counterpart with eight-layer facings. The conventional panel was cross-ply laminated with layer sequence symmetric about the middle plane of the corresponding facing, that is, $[0°/90°/0°/90°]_s$.

Table 3. Stresses and strains at the center of the upper (compressed) facing of the conventional sandwich panel.

Layer	Orientation of layer (deg.)	Z (in.)	σ_x (ksi)	σ_y (ksi)	ε_x (10^{-3})	ε_y (10^{-3})
8	0	1.000	38.572	3.67	1.430	1.280
7	90	0.995	2.935	52.53	1.410	1.190
6	0	0.900	37.588	3.39	1.390	1.110
5	90	0.985	2.809	47.84	1.380	1.030
4	90	0.980	2.746	45.50	1.360	0.944
3	0	0.975	36.112	2.98	1.340	0.861
2	90	0.970	2.620	40.81	1.320	0.778
1	0	0.965	35.128	2.70	1.310	0.695

Notes: The sign minus indicating compression is omitted. The coordinate of the upper surface of the corresponding layer is shown in the third column.

Table 4. Stresses and strains at the center of the upper (compressed) facing of the conventional sandwich panel.

Layer	Orientation of layer (deg.)	Z (in.)	σ_x (ksi)	σ_y (ksi)	ε_x (10^{-3})	ε_y (10^{-3})
12	0	1.000	33.615	2.930	1.250	1.610
11	90	0.995	2.480	40.821	1.230	1.530
10	0	0.900	32.658	2.668	1.210	1.440
9	90	0.985	2.361	36.415	1.200	1.360
8	90	0.980	31.701	2.405	1.180	1.280
7	0	0.975	2.241	32.010	1.160	1.190
6	90	0.970	2.181	29.807	1.150	1.110
5	0	0.965	30.266	2.010	1.130	1.030
4	90	0.96	2.061	25.402	1.110	0.944
3	0	0.955	29.309	1.748	1.100	0.861
2	90	0.95	1.941	20.997	1.080	0.778
1	0	0.945	28.353	1.485	1.060	0.965

Notes: The sign minus indicating compression is omitted. The coordinate of the upper surface of the corresponding layer is shown in the third column.

The results generated for the stepped and conventional panels described above were compared using the Tsai-Hill criterion to estimate the strength of the facings. According to this criterion, the stresses at every point in every layer of the facings should remain within the limitation:

$$\frac{\sigma_1^2}{s_L^2} - \frac{\sigma_1\sigma_2}{s_L^2} + \frac{\sigma_2^2}{s_T^2} + \frac{\tau_{12}^2}{s_{LT}^2} \leq 1, \tag{13}$$

where the stresses in directions 1 and 2 refer to the stresses transformed in the material coordinate system, that is, the 1-direction is oriented along the fibers, while the 2-direction is identified with the in-plane axis that is perpendicular to the fibers. The longitudinal and transverse strengths, s_L and s_T, correspond to either tension or compression, dependent on the sign of the stress in the corresponding term in Equation (13). For example, if $\sigma_1 > 0$, s_L in the first term in the left side of Equation (13) corresponds to the tensile longitudinal strength of the material. The last term in the left side of Equation (13) involves the in-plane shear strength τ_{LT}. In the following discussion, the left side of Equation (13) is called 'Tsai-Hill coefficient'. If this factor reaches the value of one in at least one of the layers, the panel is considered to fail. The efficiency of the design is improved if the Tsai-Hill coefficient in all layers of the facings is reduced. In addition to the strength of the facings discussed below, the strength of the honeycomb was checked for both conventional and stepped designs but it did not present a problem.

The conventional and stepped panels were simply supported and subjected to a uniform pressure of 470 psi chosen so that it induced failure in the outer layer of the bottom facing (see Figure 9 and layer #1 in Table 5). The largest stresses occur at the center of both conventional as well as stepped panels. The maximum stress in the sandwich plate was reduced by 10.2% as a result of stepped construction.

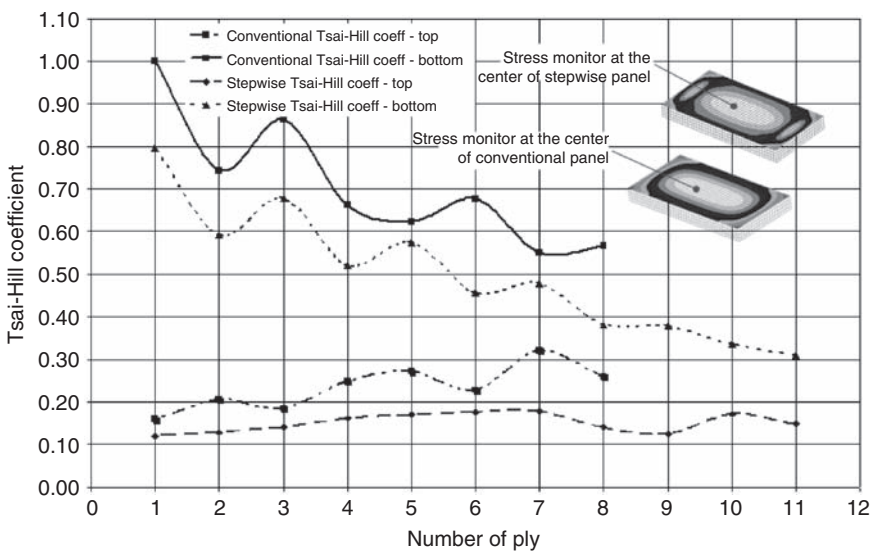

Figure 9. Tsai-Hill coefficient for conventional and three-stepped sandwich panels.

Table 5. Tsai-Hill coefficient (failure criterion) for the stresses at the center of conventional vs. stepwise panels.

Conventional panel					
Ply #	Stress monitor at center	Stress monitor at center	In-plane shear	Tsai-Hill failure criterion	Ply orient
	σ_1 (psi)	σ_2 (psi)	τ_6 (psi)	$f < 1$	
8	−51,764	−5823	4233	0.26	0
7	−3939	−83,273	4080	0.32	90
6	−50,442	−5380	3927	0.23	0
5	−3770	−75,831	3774	0.27	90
4	−3685	−72,110	3621	0.25	90
3	−48,460	−4715	3468	0.18	0
2	−3516	−64,668	3315	0.21	90
1	−47,139	−4272	3163	0.16	0
Honeycomb core	0	0	N/A	N/A	AL5056
	0	0	N/A	N/A	AL5056
	0	0	N/A	N/A	AL5056
	0	0	N/A	N/A	AL5056
	0	0	N/A	N/A	AL5056
8	47,397	3757	3181	0.57	0
7	3538	57,090	3335	0.55	90
6	48,811	4131	3488	0.68	0
5	3709	63,378	3642	0.62	90
4	3794	66,522	3795	0.66	90
3	50,930	4693	3943	0.86	0
2	3964	72,810	4102	0.74	90
1	52,343	5067	4256	1.00	0
Stepwise panel					
Ply #	Stress monitor at center	Stress monitor at center	In-plane shear	Tsai-Hill failure criterion check	Ply orient
	σ_1 (psi)	σ_2 (psi)	τ_6 (ksi)	$f < 1$	
11	−46,557	−4444	−3001	0.15	0
10	−3544	−63,562	−2825	0.17	90
9	−45,347	−4104	−2669	0.13	0
8	−3390	−57,849	−2534	0.14	90
7	−44,138	−3763	−3555	0.18	0

(continued)

Table 5. Continued

Stepwise panel					
Ply #	Stress monitor at center	Stress monitor at center	In-plane shear	Tsai-Hill failure criterion check	Ply orient
6	−3236	−52,136	−3348	0.18	90
5	−42,928	−3423	−3502	0.17	0
4	−3083	−46,423	−3307	0.16	90
3	−41,718	−3082	−3132	0.14	0
2	−2929	−40,710	−2969	0.13	90
1	−40,508	−2742	−2841	0.12	0
Honeycomb core	0	0	N/A	N/A	AL5056
	0	0	N/A	N/A	AL5056
	0	0	N/A	N/A	AL5056
	0	0	N/A	N/A	AL5056
	0	0	N/A	N/A	AL5056
11	40,962	2860	1805	0.31	0
10	2984	42,671	1887	0.34	90
9	42,172	3200	1968	0.38	0
8	3137	48,376	2074	0.38	90
7	43,382	3540	2601	0.48	0
6	3291	54,081	2729	0.46	90
5	44,592	3879	2955	0.57	0
4	3445	59,787	3084	0.52	90
3	45,801	4219	3257	0.68	0
2	3598	65,492	3455	0.59	90
1	47,011	4559	3655	0.80	0

Note: f is function of Tsai-Hill failure criterion.

Even more remarkable, the left side of inequality (13) called in Table 1 and Figure 9, the Tsai-Hill coefficient was reduced by 20%. These improvements achieved at the expense of a small weight increase (3.1%) confirm potential benefits of stepped panels.

Even in the case of a uniform pressure applied to a sandwich panel with stepped facings, the location of failure may be 'shifted' from the center of the panel to the region of an abrupt transition in the facing thickness. The stresses at two critical locations in the transition region are shown in Table 6 and Figure 10. As follows from the comparison with Table 5 and Figure 9, the failure of the panels analyzed in these examples occurs at the center, rather than at the

Table 6. Tsai-Hill coefficient at point 1 and 2 of stepwise panel (see Figure 10).

Stepwise panel					
Ply #	Stress monitor at point 1	Stress monitor at point 1	In-plane shear	Tsai-Hill failure criterion	Ply orient
	σ_1 (psi)	σ_2 (psi)	τ_6 (ksi)	$f < 1$	
7	−32,576	−2131	−3555	0.15	0
6	−2213	−28,399	−3348	0.13	90
5	−30,806	−2022	−3502	0.15	0
4	−2091	−26,928	−3307	0.13	90
3	−29,035	−1912	−3132	0.12	0
2	−1969	−25,457	−2969	0.11	90
1	−27,265	−1803	−2841	0.10	0
Honeycomb core	0	0	N/A	N/A	AL5056
	0	0	N/A	N/A	AL5056
	0	0	N/A	N/A	AL5056
	0	0	N/A	N/A	AL5056
	0	0	N/A	N/A	AL5056
7	27,834	1977	2601	0.20	0
6	2046	28,393	2729	0.22	90
5	29,642	2087	2955	0.24	0
4	2170	29,855	3084	0.25	90
3	31,450	2196	3257	0.27	0
2	2294	31,317	3455	0.30	90
1	33,258	2306	3655	0.32	0
Stepwise panel					
Ply #	Stress monitor at point 2	Stress monitor at point 2	In-plane shear	Tsai-Hill failure criterion	Ply orient
	σ_1 (psi)	σ_2 (psi)	τ_6 (ksi)	$f < 1$	
7	−26,237	−3039	−3555	0.15	0
6	−2125	−43,870	−3348	0.16	90
5	−23,739	−2545	−3502	0.14	0
4	−1881	−36,816	−3307	0.14	90
3	−23,413	−2315	−3132	0.11	0
2	−1803	−32,833	−2969	0.11	90
1	−23,087	−2086	−2841	0.10	0
	0	0	N/A	N/A	AL5056

(continued)

Table 6. Continued

	Stepwise panel				
Ply #	Stress monitor at point 2	Stress monitor at point 2	In-plane shear	Tsai-Hill failure criterion	Ply orient
Honeycomb core					
	0	0	N/A	N/A	AL5056
	0	0	N/A	N/A	AL5056
	0	0	N/A	N/A	AL5056
	0	0	N/A	N/A	AL5056
7	25,285	2038	2601	0.20	0
6	1939	33,394	2729	0.21	90
5	23,687	2509	2955	0.29	0
4	1948	40,249	3084	0.24	90
3	24,015	2746	3257	0.34	0
2	2028	44,356	3455	0.28	90
1	24,343	2983	3655	0.41	0

Note: f is function of Tsai-Hill failure criterion.

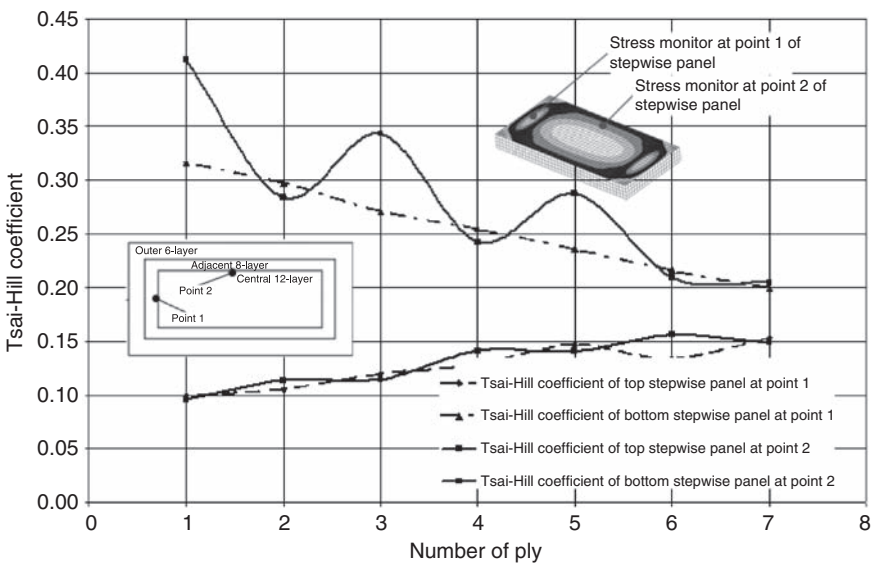

Figure 10. Tsai-Hill coefficient for points 1 and 2 of the three-stepped sandwich panel points are identified in the figure.

transition region. However, the situation can change, dependent on the design of transition and the overall dimensions of the stepped regions of the panel.

Conclusions

A potential for design of sandwich panels with stepped facings has been investigated. It appears that stepped facings may provide a significant benefit reducing bending stresses in the facings and increasing the load-carrying capacity of sandwich panels. Such design may also prove advantageous in sandwich structures where the mode of failure is buckling. These advantages are further reinforced by the observation that the manufacture of such panels does not involve significant complications compared to conventional sandwich structures. A further research might concentrate on the optimization of the stepped design aiming at achieving desirable strength or stiffness subject to prescribed weight limitations.

In addition, the feasibility of using solutions based on the first-order theory for the analysis of sandwich panels with a commercially available aluminum honeycomb core was considered. As was shown through the comparison of deflections and stresses generated by the analytical first-order theory solution with finite element results accounting for 3D effects, the theory remains sufficiently accurate, even at the width-to-thickness ratio of 20. Therefore, it is concluded that commercially available honeycomb cores will often be 'stiff enough' to justify the application of the first-order theory to the analysis of typical sandwich structures. This observation may become invalid in the case of panels with a 'softer' polymeric core or in the case of concentrated loads resulting in local 3D effects.

Acknowledgements

This research was supported by Boeing that provided necessary technical and computational resources. The discussions with Professor George A. Kardomateas (Georgia Institute of Technology) are warmly appreciated.

References

1. Birman V and Byrd LW. Modeling and Analysis of Functionally Graded Materials and Structures. *Applied Mechanics Reviews* 2007; 60: 195–216.
2. Birman V, Simitses GJ and Shen L. Stability of Short Sandwich Cylindrical Shells with Rib-reinforced Facings. In: Katsikadelis J.T, Beskos D.E and Gdoutos EE (eds) *Recent Advances in Applied Mechanics*. Greece: National Technical University of Athens, 2000, p.11–21.
3. Gupta AP and Sharma KP. Bending of a Sandwich Annular Plate of Variable Thickness. *Indian Journal of Pure and Applied Mathematics* 1982; 13: 1313–1321.
4. Paydar N and Libove C. Stress Analysis of Sandwich Plates of Variable Thickness. *Journal of Applied Mechanics* 1988; 55: 419–424.
5. Libove C and Lu C-H. Beamlike Bending of Variable-thickness Sandwich Plates. *AIAA Journal* 1989; 12: 1617–1618.
6. Lu C-H and Libove C. Beamlike Harmonic Vibration of Variable-thickness Sandwich Plates. *AIAA Journal* 1991; 29: 299–305.

7. Lu C-H. Bending of Anisotropic Sandwich Beams with Variable Thickness. *Journal of Thermoplastic Composite Materials* 1994; 7: 364–374.
8. Peled D and Frostig Y. High-order Bending of Sandwich Beams with Variable Flexible Core and Nonparallel Skins. *ASCE Journal of Engineering Mechanics* 1994; 120: 1255–1269.
9. Vel SS, Cacesse, V and Zhao, H. (2002). Modeling and Analysis of Tapered Sandwich Beams, In: *Proceedings of the American Society for Composites*, *Seventeenth Annual Technical Conference*, Purdue Fort Lafayette, Indiana, 21–23 October.
10. Vel SS, Cacesse V and Zhao H. Elastic Coupling Effects in Tapered Sandwich Panels with Laminated Anisotropic Composite Facings. *Journal of Composite Materials* 2005; 39: 2161–2183.
11. Reddy JN. *Mechanics of Laminated Composite Plates and Shells. Theory and Analysis*, 2nd edn. Boca Raton: CRC Press, 2004.
12. Noor AK. Finite Element Buckling and Postbuckling Analyses. In: Turvey G.J and Marshall I.H (eds) *Buckling and Postbuckling of Composite Plates*. London: Chapman & Hall, 1995, p.58–107.
13. Li R and Kardomateas GA. Nonlinear High-order Core Theory for Sandwich Plates with Orthotropic Phases. *AIAA Journal* 2008; 46: 2926–2934.
14. Sokolinsky V and Frostig Y. Branching Behavior in the Nonlinear Response of Sandwich Panels with a Transversely Flexible Core. *International Journal of Solids and Structures* 2000; 37: 5745–5772.
15. Frostig Y, Thomsen OT and Sheinman I. On the Non-linear Theory of Unidirectional Sandwich Panels with a Transversely Flexible Core. *International Journal of Solids and Structures* 2005; 42: 1443–1463.
16. Whitney JM. *Structural Analysis of Laminated Anisotropic Plates*. Lancaster: Technomic, 1987.
17. Vinson JR. *The Behavior of Sandwich Structures of Isotropic and Composite Materials*. Lancaster: Technomic, 1999.
18. Birman V and Bert CW. On the Choice of Shear Correction Factor in Sandwich Structures. *Journal of Sandwich Structures and Materials* 2002; 4: 83–95.